Long-term sea level trends: Natural or anthropogenic?

M Becker, Mikhail Karpytchev, S Lennartz-Sassinek

AGU PUBLICATIONS

Geophysical Research Letters

RESEARCH LETTER
10.1002/2014GL061027

Key Points:
- Long-term persistence impacts on sea level rise estimation
- Sea level change is clearly unnatural in two thirds of the longest tidal records
- Sea level change magnitude cannot be explained without human influence

Supporting Information:
- Readme
- Figure S1
- Figure S2
- Table S1

Correspondence to:
M. Becker,
melanie.becker@ird.fr

Citation:
Becker, M., M. Karpytchev, and S. Lennartz-Sassinek (2014), Long-term sea level trends: Natural or anthropogenic?, *Geophys. Res. Lett.*, *41*, doi:10.1002/2014GL061027.

Received 27 JUN 2014
Accepted 18 JUL 2014
Accepted article online 23 JUL 2014

Long-term sea level trends: Natural or anthropogenic?

M. Becker[1], M. Karpytchev[2], and S. Lennartz-Sassinek[3]

[1]ESPACE-DEV UMR 228 UAG/IRD, Cayenne, French Guiana, [2]LIENSs UMR 7266 CNRS, University of La Rochelle, France, [3]Institute for Geophysics and Meteorology, University of Cologne, Germany

Abstract Detection and attribution of human influence on sea level rise are important topics that have not yet been explored in depth. We question whether the sea level changes (SLC) over the past century were natural in origin. SLC exhibit power law long-term correlations. By estimating Hurst exponent through Detrended Fluctuation Analysis and by applying statistics of *Lennartz and Bunde* [2009], we search the lower bounds of statistically significant external sea level trends in longest tidal records worldwide. We provide statistical evidences that the observed SLC, at global and regional scales, is beyond its natural internal variability. The minimum anthropogenic sea level trend (MASLT) contributes to the observed sea level rise more than 50% in New York, Baltimore, San Diego, Marseille, and Mumbai. A MASLT is about 1 mm/yr in global sea level reconstructions that is more than half of the total observed sea level trend during the XXth century.

1. Introduction

Understanding the causes of the observed rise in mean sea level [*IPCC AR5*, 2013] is of primary concern for the climate projections and evaluation of vulnerability of coastal communities. *Church and White* [2011] have estimated a global mean sea level (GMSL) linear trend of 1.7 mm/yr in the sea level measurements during the 20th century. However, sea level rise is far from being a uniform process [*Church et al*., 2004; *Jevrejeva et al*., 2006; *Cazenave and Llovel*, 2010; *Nerem et al*., 2010; *Becker et al*., 2012]. Instead, it shows strong spatial and temporal regional patterns that can deviate substantially from global averages, to the point that local and global trends differ in sign at some locations [*Stammer et al*., 2013]. From a physical point of view, the sea level variations are driven by changes of ocean water volume due to ocean-mass addition, oceanic warming, and by the deformation of the solid Earth changing the shape of oceanic basins [*Mitchum et al*., 2010]. From the perspective of assessing the contribution of human activities to climate changes, the sea level drivers can be partitioned in anthropogenic and natural forcing [*Hegerl et al*., 2010]. Following *Bloomfield and Nychka* [1992], *Hasselmann* [1993], *Hegerl et al*. [1996], *Zwiers* [2005], and *Zorita et al*. [2008], we have reformulated this question by asking: how large a sea level trend could be expected as result of natural internal variability? In order to answer it, we have applied a method developed recently by *Lennartz and Bunde* [2009, 2011, 2012] for detecting anthropogenic influence in time series with long-term power law correlations. The sea level fluctuations result from complex interactions between diverse physical processes and, as many other geophysical signals, exhibit long-term correlations [*Agnew*, 1992] that can be effectively modeled as outcomes of stochastic power law process with a Hurst exponent $\alpha > 0.5$ [*Beretta et al*., 2005; *Barbosa et al*., 2008; *Bos et al*., 2013]. The Hurst exponent $\alpha > 0.5$ indicates the presence of long-term correlations that manifest themselves as persistent low-frequency oscillations [*Feder*, 1988; *Rybski and Bunde*, 2009]. In long-term correlated records, large events well above the average are more likely to be followed by large events, and small events well below the average by small events [*Hurst et al*., 1965; *Mandelbrot and Wallis*, 1968, 1969]. In other words, a period of a low stand of the sea level is more likely to be followed by a low sea level whereas a high sea level is more probably followed by a high one. This persistence holds, in theory, on over all time scales and may look like positive or negative trends in the sea level data. Distinguishing between these trend-like natural oscillations and the external trends in the longest available sea level records is the principal goal of this study.

2. Data and Methods

First, we analyze two GMSL reconstructions: one obtained by *Jevrejeva et al*. [2006] (GMSLR06 hereafter) for the period 1807–2002 (available from: http://www.psmsl.org/products/reconstructions/jevrejevaetal2006.php) and another computed by *Church and White* [2011] (GMSLR11 hereafter) for the period 1880–2009

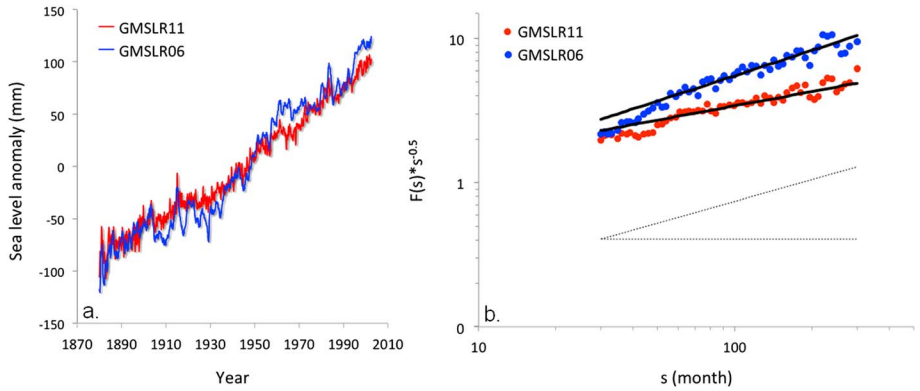

Figure 1. Global mean sea level changes: (a) Time series of monthly GMSLR from *Jevrejeva et al.* [2006] (GMSLR06 blue curve) and *Church and White* [2011] (GMSLR11 red curve). (b) Fluctuation function of second-order detrended fluctuation analysis (DFA2). The straight lines are the best fits between s = 60 and s = 180 months.

(available from: http://www.cmar.csiro.au/sealevel/sl_data_cmar.html). *Jevrejeva et al.* [2006] have combined 1023 RLR (Revised Local Reference) monthly tide-gauge records from the Permanent Service for Mean Sea Level database [*PSMSL*, 2014; *Holgate et al.*, 2013] by using a virtual station method of averaging neighboring station sea level changes in several regions and then obtaining the global mean sea level change. *Church and White* [2011] have used monthly tide-gauge data from the PSML by using spatial patterns of empirical orthogonal functions estimated from the satellite altimetry data set. In both reconstructions, the tide-gauge records were priorly corrected for vertical land movement induced by Glacial Isostatic Adjustment (GIA). In order to be consistent with the rest of the study, we consider the GMSL reconstructions over their common 112 year period from 1880 to 2002 (Figure 1a). In addition, to take a closer look at the regional sea level variations, we analyze 59 long-term monthly mean tide-gauge records (Figure 2 and Table 1) included in the RLR data set of the PMSL. We select tide-gauge records with at least 100 years of data, with exception of the Newlyn, Brest, and Batiscan records (~98 years), and with small gaps (≤4 consecutive years). We have corrected the tide-gauge time series for the GIA effect using the ICE-5G (VM2) model from *Peltier* [2004]. For a variety of reasons [changes in instrumentation, earthquakes, or other natural of anthropogenic factors; see *Becker et al.*, 2009], the gaps and discontinuities can strongly affect tide-gauge time series. Missing data in small gaps (≤4 consecutive years) have been reintroduced by linear interpolation. For all considered time series, the seasonal variations have been removed by subtracting the mean values for each calendar month and dividing the data by the seasonal standard deviations [*Koscielny-Bunde et al.*, 2006; *Lennartz and Bunde*, 2009]. Figure 3a shows the deseasonalized records for some representative stations. In each deseasonalized GIA-corrected sea level time series, we estimate three parameters: (1) the Hurst exponent α, (2) the relative increase of sea level, x, and (3) the possible external SLC, Δ_{ext}, during the given period. To determine α, we use the second-order detrended fluctuation analysis (DFA2) that removes the influence of linear trends on the determination of α [*Kantelhardt et al.*, 2001]. In the following, we present briefly the main steps of the n-order DFA procedure for a record $X(i)$, $i = 1 \ldots L$. First, we determine the number of intervals of equal length $L_s = \lfloor L/s \rfloor$ and integrate the record: $y(k) = \sum_{k=1}^{L} X_k - \langle X \rangle$, where $\langle X \rangle$ is the data mean. Next, we divide the integrated time series into L_s non-overlapping intervals. In each interval, we fit the integrated time series by using a n-order polynomial function, $p_v(k)$ with v a time window of size $s(v = 1, \ldots, L_s)$, which is regarded as the local trend. In each interval, we subtract it to get the detrended fluctuations: $y_v(k) = y(k) - p_v(k)$. The variance of this integrated and detrended time series is calculated by: $F_v^2(s) = \frac{1}{s} \sum_{k(v)=1}^{s} y_v(k)^2$. This computation is repeated over all time scales to provide the fluctuation function: $F(s) = \sqrt{\frac{1}{L_s} \sum_{v=1}^{L_s} F_v^2(s)}$. These fluctuations can be characterized by the fluctuation exponent α, the slope of the line relating $ln(F(s))$ to $ln(s)$.

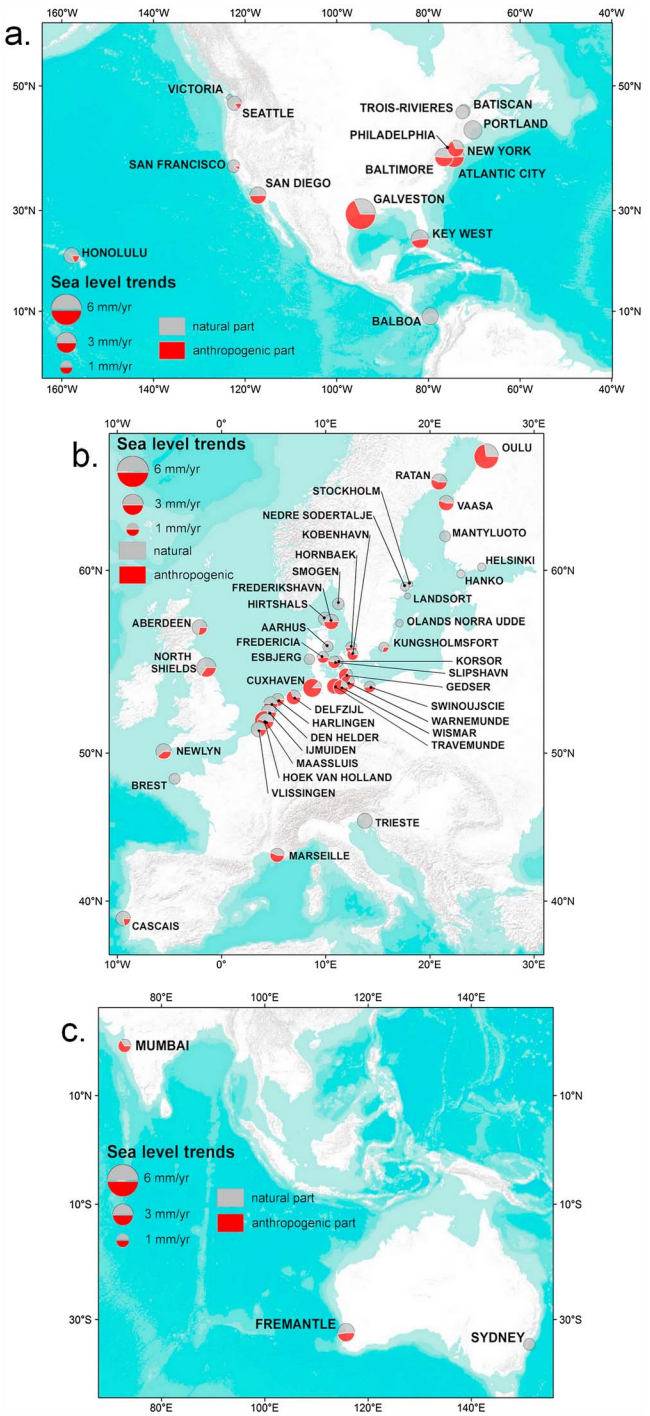

Figure 2. Minimum antropogenic contribution and maximum natural component of the observed sea level trend: (a) Northwest Pacific and Northeastern Atlantic, (b) European Atlantic, North, and the Baltic Seas, and (c) Indian Ocean and Australia. Each circle represents a gauge location and is color coded to reflect the maximum natural and minimum anthropogenic part of the sea level trend. Basemap from ESRI, Inc.

To determine x, we estimate (1) the sea level change Δ_{obs} as a difference between the end point and the beginning of the regression line drawn over considered time interval and (2) the standard deviation of sea level, σ_t, around this regression line. Then, the relative sea level increase is defined as a dimensionless ratio $x = \Delta_{obs}/\sigma_t$. *Lennartz and Bunde* [2009, 2011, 2012] have found the probability density function $P(x, \alpha; L)$ of a relative increase of magnitude x in a power law series of length L with the Hurst exponent α. The integration of $P(x, \alpha; L)$ leads to the exceedance probability $W(x, \alpha; L) = \int_x^\infty P(x', \alpha; L)dx'$ that is the probability of observing a relative increase greater than x in a pure power law correlated series. In our study, the question whether the observed sea level change (SLC) does occur naturally turns to a statistical decision problem: whether the measured x exceeds or not the bounds of the confidence interval $[-x_Q, +x_Q]$. Here $x_Q = W^{-1}((1-Q)/2, \alpha; L)$ and Q is the confidence level of testing the null-hypothesis "the observed x is of natural origin". Below, we set the bounds x_Q of a rather conservative acceptance region: $Q = 0.99$ (the results corresponding to a $Q = 0.95$ can be found in the supporting information). It means that if x exceeds the boundaries x_Q, then the trend is significantly anthropogenic at 99%. But if it does not exceed these thresholds, we cannot decide whether the anthropogenic sea level trend is present or not. It might be, for example, that a natural decrease together with an anthropogenic increase is adding up to a seemingly harmless behavior. Ultimately, the contribution of the minimum anthropogenic sea level trend (MASLT) Δ_{ext}/L contribution to the observed sea level trend Δ_{obs}/L, corresponding to a total sea level increase Δ_{obs}, is given by: $\Delta_{ext} = \sigma_t(x - x_Q)$ (see Figure SM2 in the supporting information). In our analysis, we chose sea level records longer than $L > 1200$ months because the error in the

Geophysical Research Letters

10.1002/2014GL061027

Table 1. Summary of Tide-Gauge Stations and GMSLR[a]

PSMSL ID	Station Name	Location		Years of Data	Percentage of Gaps	L	GIA	$\Delta obs / L$				$\Delta ext / L$
		Longitude	Latitude	Start–End	(Max. Gap Size in Months)	(Months)	(mm/yr)	(mm/yr)	α	x	x_Q 99%	(mm/yr)
Global Mean Sea Level												
	GMSLR06			1880–2002	–	1470	–	1.7	1.08 ± 0.09	13.7	6.2	1.0
	GMSLR11			1880–2002	–	1470	–	1.5	0.83 ± 0.07	20.0	2.2	1.3
North Atlantic Europe												
202	Newlyn	50.1	−5.5	1915–2012	1% (7)	1172	0.3	1.5	0.70 ± 0.05	2.1	1.2	0.6
1	Brest	48.4	−4.5	1846–1943	4% (48)	1176	0.2	0.8	0.72 ± 0.11	0.8	1.7	–
52	Cascais	38.7	−9.4	1882–1993	7% (36)	1344	−0.1	1.4	0.81 ± 0.07	2.8	2.1	0.3
North Sea												
179	Smogen	58.4	11.2	1911–2012	–	1224	−2.7	0.9	0.67 ± 0.09	0.9	1.2	–
89	Hirtshals	57.6	10.0	1892–2012	4% (27)	1452	−1.3	1.1	0.68 ± 0.06	1.2	1.0	0.2
91	Frederikshavn	57.4	10.5	1894–2012	3% (17)	1428	−1.3	1.4	0.64 ± 0.08	2.0	0.9	0.7
21	Aberdeen II	57.2	−2.1	1862–1965	–	1248	−0.8	1.4	0.72 ± 0.09	2.2	1.5	0.4
76	Aarhus	56.1	10.2	1888–2012	2% (12)	1492	−0.1	0.7	0.75 ± 0.08	1.3	1.6	–
119	Hornbaek	56.1	12.5	1891–2012	2% (6)	1464	−0.4	0.8	0.56 ± 0.05	1.0	0.5	0.4
81	Fredericia	55.6	9.8	1889–2012	1% (3)	1481	0.3	0.8	0.64 ± 0.07	2.0	0.9	0.4
80	Esbjerg	55.5	8.4	1889–2012	1% (7)	1488	0.5	0.7	0.65 ± 0.08	0.5	0.9	–
113	Korsor	55.3	11.1	1897–2012	2% (5)	1392	0.1	0.8	0.68 ± 0.11	1.3	1.3	–
98	Slipshavn	55.3	10.8	1896–2012	3% (12)	1404	0.1	0.9	0.62 ± 0.06	1.7	0.7	0.5
95	North Shields	55.0	−1.4	1895–2012	6% (43)	1416	−0.4	2.3	0.89 ± 0.09	4.5	3.0	0.8
7	Cuxhaven 2	53.9	8.7	1843–2010	–	2016	0.4	2.2	0.49 ± 0.05	2.5	0.3	1.9
24	Delfzijl	53.3	6.9	1865–2012	–	1776	0.4	1.3	0.58 ± 0.05	1.6	0.5	0.9
25	Harlingen	53.2	5.4	1865–2012	–	1776	0.4	1.0	0.59 ± 0.05	1.3	0.5	0.6
23	Den Helder	53.0	4.7	1865–2012	–	1776	0.3	1.2	0.67 ± 0.06	1.8	0.9	0.6
32	Ijmuiden	52.5	4.6	1871–2012	–	1700	0.2	1.4	0.79 ± 0.04	2.1	1.5	0.4
22	Hoek Van Holland	52.0	4.1	1864–2012	–	1788	0.0	2.4	0.67 ± 0.05	4.2	0.8	1.9
9	Maassluis	51.9	4.2	1848–2012	–	1980	0.0	1.6	0.76 ± 0.05	2.8	1.3	0.9
20	Vlissingen	51.4	3.6	1862–2012	–	1812	−0.1	1.5	0.81 ± 0.08	2.5	1.9	0.3
Baltic Sea												
79	Oulu	65.0	25.4	1889–2012	5% (8)	1488	−10.0	3.7	0.61 ± 0.07	2.7	0.7	2.7
88	Ratan	64.0	20.9	1892–2012	<1% (2)	1452	−9.4	1.6	0.56 ± 0.04	1.2	0.5	0.9
57	Vaasa	63.1	21.6	1883–2012	5% (21)	1552	−8.7	1.4	0.53 ± 0.05	1.1	0.4	0.8
172	Mantyluoto	61.6	21.5	1910–2012	2% (7)	1229	−6.5	0.7	0.53 ± 0.05	0.4	0.4	–
14	Helsinki	60.2	25.0	1879–2012	<1% (1)	1608	−2.0	−0.3	0.53 ± 0.05	−0.2	0.4	–
71	Hanko	59.8	23.0	1887–1997	7% (34)	1322	−2.5	−0.3	0.68 ± 0.09	−0.1	1.2	–
78	Stockholm	59.3	18.1	1889–2012	–	1488	−4.0	0.2	0.57 ± 0.06	0.2	0.6	–
31	Nedre Sodertalje	59.2	17.6	1869–1970	–	1224	−3.9	0.5	0.41 ± 0.06	–	–	–
68	Landsort	58.7	17.9	1887–2005	–	1428	−3.1	0.2	0.53 ± 0.06	0.1	0.4	–
69	Olands Norra Udde	57.4	17.1	1887–2012	–	1512	−1.4	0.3	0.48 ± 0.05	0.3	0.3	–
70	Kungsholmsfort	56.1	15.6	1887–2012	<1% (1)	1512	−0.6	0.6	0.52 ± 0.05	0.6	0.4	0.2
82	Kobenhavn	55.7	12.6	1889–2012	2% (7)	1488	−0.3	0.8	0.51 ± 0.06	1.1	0.4	0.5
120	Gedser	54.6	11.9	1892–2012	1% (2)	1452	0.0	1.2	0.45 ± 0.05	1.6	0.2	1.0
11	Warnemunde 2	54.2	12.1	1855–2012	<1% (2)	1893	−0.1	1.3	0.55 ± 0.05	2.4	0.4	1.1
13	Travemunde	54.0	10.9	1856–1984	–	1548	0.1	1.5	0.53 ± 0.05	2.5	0.4	1.3
2	Swinoujscie	53.9	14.2	1811–1944	<1% (7)	1608	−0.3	0.8	0.58 ± 0.05	1.0	0.5	0.4
8	Wismar 2	53.9	11.5	1848–2012	<1% (2)	1974	0.0	1.4	0.62 ± 0.05	2.8	0.6	1.1
North Pacific America												
166	Victoria	48.4	−123.4	1909–2012	1% (10)	1246	0.4	0.2	0.89 ± 0.07	0.3	2.9	–
127	Seattle	47.6	−122.3	1899–2012	<1% (1)	1368	0.7	1.3	0.79 ± 0.07	2.2	1.9	0.2

Table 1. (continued)

PSMSL ID	Station Name	Location		Years of Data	Percentage of Gaps (Max. Gap Size in Months)	L (Months)	GIA (mm/yr)	$\Delta obs/L$ (mm/yr)	α	x	x_Q 99%	$\Delta ext/L$ (mm/yr)
		Longitude	Latitude	Start–End								
10	San Francisco	37.8	−122.5	1854–2012	<1% (2)	1902	0.4	1.0	0.86 ± 0.06	2.5	2.2	0.1
158	San Diego	32.7	−117.2	1906–2012	2% (9)	1284	0.2	1.8	0.81 ± 0.08	4.5	2.2	0.9
155	Honolulu	21.3	−157.9	1905–2012	–	1296	−0.2	1.6	0.86 ± 0.08	3.4	2.7	0.3
163	Balboa	9.0	−79.6	1908–2009	1% (3)	1224	−0.2	1.8	0.89 ± 0.14	3.0	3.8	–
North Atlantic America												
144	Batiscan	46.5	−72.3	1913–2012	26% (11)	1195	−1.4	1.1	0.86 ± 0.09	−0.1	2.9	–
126	Trois-Rivieres	46.3	−72.6	1912–2012	6% (9)	1205	−1.5	1.1	0.85 ± 0.08	0.0	2.6	–
183	Portland	43.7	−70.2	1912–2012	<1% (2)	1212	−0.3	2.1	0.96 ± 0.10	4.3	4.3	–
12	New York	40.7	−74.0	1893–2012	1% (4)	1440	1.3	1.8	0.69 ± 0.07	3.5	1.1	1.2
135	Philadelphia	39.9	−75.1	1900–2012	3% (16)	1350	1.3	1.7	0.76 ± 0.07	2.3	1.7	0.4
180	Atlantic City	39.4	−74.4	1911–2012	7% (23)	1216	1.3	2.8	0.86 ± 0.08	4.5	2.7	1.1
148	Baltimore	39.3	−76.6	1902–2012	<1% (2)	1326	1.0	2.1	0.76 ± 0.10	4.0	1.9	1.1
Gulf of Mexico												
161	Galveston II	29.3	−94.8	1908–2012	1% (4)	1256	0.3	6.0	0.84 ± 0.08	8.0	2.5	4.1
188	Key West	24.6	−81.8	1913–2012	1% (8)	1200	0.1	2.2	0.81 ± 0.10	4.6	2.4	1.0
Indian Ocean												
43	Mumbai	18.9	72.8	1878–1994	1% (4)	1398	−0.3	1.1	0.61 ± 0.08	2.3	0.8	0.7
Mediterranean Sea												
154	Trieste	45.6	13.8	1901–2012	5% (36)	1344	−0.1	1.4	0.83 ± 0.09	1.8	2.4	–
61	Marseille	43.3	5.4	1885–2012	3% (22)	1535	0.0	1.2	0.67 ± 0.09	2.5	1.1	0.7
Australia												
111	Fremantle	−32.1	115.7	1897–2012	8% (30)	1392	−0.3	1.9	0.76 ± 0.07	3.0	1.6	0.9
65	Sydney	−33.9	151.2	1886–1993	–	1296	−0.2	0.8	0.86 ± 0.06	1.7	2.5	–

[a]Name, location, years of data used, percentage of gaps, length in months, Glacial Isostatic Adjustment (GIA) corrections, and sea level trend of the tide-gauge records selected from the PSMSL. The Hurst exponent α is given with its relative standard error (95% confidence level). Here $\Delta_{ext}/L = "-"$, if the observed relative trend x is inside the corresponding confidence interval $[-x_Q, +x_Q]$ and is thus not significant.

determination of α by DFA2 in shorter series gets larger [*Kantelhardt et al.*, 2001]. Figures 1b and 3b show the results of this analysis for GMSL reconstructions and for some representative stations. The obtained values of Δ_{obs}, x, α, N, and Δ_{ext} are listed in the Table 1. Here, we fitted α between scales $s = 60$ and $s = 180$ months, corresponding to 5 and 15 years. We skipped fitting at shorter scales to avoid the influence of short-range memory and the larger scales because of statistical fluctuations of the detrended fluctuation function on these scales.

3. Results

3.1. Regional Sea Level

The important question arises here about how does the interplay between the internal climate variability and anthropogenic influence manifest itself in regional variations of SLC?

The Hurst exponent α varies significantly from one region to another reflecting mainly local/regional phenomena as demonstrated by *Barbosa et al.* [2008], *Hughes and Williams* [2010], and *Bos et al.* [2013]. The largest observed values of $\alpha \sim 0.9$ have been found in the north Pacific sea level records from Balboa, in Panama, to Victoria, in Canada and somewhat smaller $\alpha \sim 0.8$ in Seattle and San Diego (Table 1). An unnatural SLC is observed in four out of six sea level records: Seattle, San Francisco, San Diego, and Honolulu (Figure 2a). In San Diego, the MASLT is 0.9 mm/yr, or about 50% of the observed sea level trend. For other tide gauges, the estimated part of the MASLT is significantly lower and represents only 10–20% of the observed sea level trend. These results confirm *Meyssignac et al.* [2012] observations that the sea level fluctuations in the Tropical Pacific are due mostly to the internal modes of ocean variability.

In the Western North Atlantic, two regions can be distinguished: The first one includes the Trois-Rivieres and Batiscan tide gauges both located on the northern shore of the Saint Lawrence River, Canada, and Portland tide gauge, in the U.S. For these tide gauges, α is large (ranging between 0.8 and 1, Table 1). None of these three records shows a significant unnatural SLC over their period of operation (Figure 2a). It is important to note here that the tide gauges located in the Saint Lawrence River estuary are influenced by strong discharge from upland runoff, in addition to sea level influences. Thus, the sea level variability enhanced by the estuarine dynamics makes the external trends to go undetected even with a rather conservative choice of the 99% confidence level. The second region stands

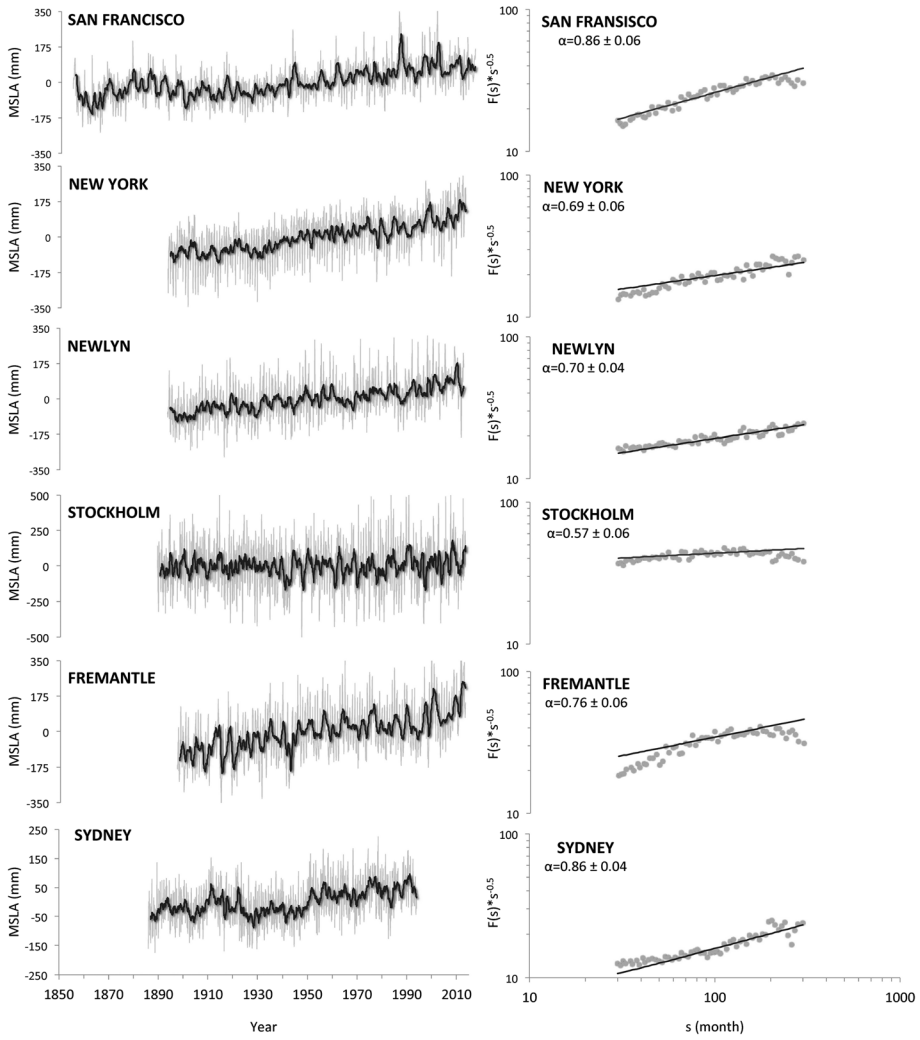

Figure 3. Tide-gauge sea level changes: (a) Time series of monthly sea level anomaly (MSLA) for six representative tide-gauge records. The bold black lines are the 12 month-running mean window sea level anomaly. (b) Fluctuation function of DFA2 for the deseasonalized detrended data sets (dotted symbols). The straight lines are the best fits between s = 60 and s = 180 months.

out as a cluster of unnatural SLC in the largest urban areas of the US East Coast: New York, Philadelphia, Atlantic City, and Baltimore (Figure 2a). In New York, the minimum externally driven sea level trend is 1.2 mm/yr, or about 67% of the observed total sea level trend. At the Atlantic City and Baltimore tide gauges, the estimated part of the MASLT is 1.1 mm/yr and represents 39% and 52% of the total sea level trend, respectively. For the tide gauge at Philadelphia, the estimated part of the MASLT is lower and represents 24% of the observed sea level trend. Here again, this lower value can be explained by the location of Philadelphia tide gauge at about 100 km upstream from the Delaware River mouth. These cities correspond to the sea level rise "hot spot" detected by *Sallenger et al.* [2012]: a region where the sea level is rising between three and four times faster than the global average. Our analysis indicates unnatural origin of this fast sea level rising due probably to the anthropogenic warming that induces, among other consequences, significant changes in the strength of the Atlantic Meridional overturning circulation and of the Gulf Stream [*Sallenger et al.* 2012].

In the northern Gulf of Mexico, a strong significant unnatural SLC is found at Galveston (Figure 2a). The MASLT is 4.1 mm/yr (i.e., 68%) against 6 mm/yr of the observed sea level trend. This tide gauge is known to be dominated by land subsidence due to the extraction of subsurface fluids, hydrocarbons, and groundwater withdrawal [*Morton et al.*, 2006; *Kolker et al.*, 2011]. In contrast, the Key West sea level station is situated on a stable coral reef, at the edge of the Florida shelf [*Maul and Martin*, 1993; *Davis*, 2011], and little affected by

the post-glacial rebound. The MASLT at Key West station is 1 mm/yr and represents 45% of the observed sea level trend. Detecting a significant unnatural SLC at Key West indicates probably unnatural trend in dynamics of the Loop Current flowing out the Gulf of Mexico to the western North Atlantic.

Along the Atlantic coasts of Iberia and UK the tide gauges of Newlyn and Cascais present α in range [0.7; 0.8] and significant unnatural SLC (Figure 2b). The MASLT is 0.6 mm/yr at Newlyn tide gauge and 0.3 mm/yr at Cascais tide gauge, or about 40% and 21% of the observed sea level trend, respectively. It is tentative to make a parallel with the observed "hot spot" at the east coast of U.S., following *Miller and Douglas* [2007] and *Woodworth et al*. [2010] who have suggested a link between sea level at the eastern and western boundaries of the North Atlantic through changes in the strength of the oceanic subtropical gyre. It is remarkable that the Brest record, French Atlantic Coast, being coherent with the regional value $\alpha \sim 0.7$ does not show a significant SLC. This might be explained by the earlier period of the Brest record (1846–1943) considered in the study, as compared to the Newlyn and Cascais records. Also of interest is the comparison of Portland (Maine) and Cascais sea level records that have been shown [*Miller and Douglas*, 2007; *Stammer et al*., 2013] to display similar sea level variations but shifted in time by about 10 years. Whereas the sea level trend at Cascais is identified as having an unnatural component, that at Portland can still be explained by its natural power law variability.

In the Mediterranean Sea, the century-scale tide record from Marseille reveals a strong unnatural SLC (Figure 2b). The MASLT is 0.7 mm/yr, or more than a half (58%) of the total sea level trend. Contrarily, the Trieste tide-gauge record shows no significant unnatural SLC over the period of operation although its fluctuation exponent ($\alpha \sim 0.8$) is close to that in Marseille ($\alpha \sim 0.7$). This difference indicates a stronger regional/local driver of SLC at Marseille.

In the North Sea, the relative sea level increase is observed at all tide gauges (Figure 2b), and it is significantly larger than can be expected from the natural sea level variability. Although, there are no long-term Norwegian records used in our analysis, it seems reasonable to suppose that the whole North Sea has a large contribution of unnatural SLC. In the straits between the North Sea and the Baltic Sea (Hornbaek, Smogen, Hirtshal, Frederikshavn, Aarhus, Fredericia, Korsor, and Slipshavn), we find homogeneous distribution of α in range [0.6; 0.7] (Table 1).

The Baltic Sea is a semi-enclosed sea consisting of three well-defined sub-basins: The Bothnian Bay, the Bothnian Sea, and the Baltic proper with the Gulf of Finland. In the extreme western part of the Baltic Sea, the tide gauges of Travemunde, Wismar 2, Warnemunde 2, Gedser, and Swinoujscie show α in range [0.5; 0.6] and strong significant unnatural SLC (Figure 2b). In this region, the MASLT represent more than 80% of the observed sea level trends, except for Swinoujscie and Kobenhavn, where the MASLT represent 50% and 63% of the observed sea level trend, respectively. The central region that includes the Bothnian Sea, the Finland Gulf, and the proper Baltic Sea shows, in average, coherent Hurst exponents in the range [0.5; 0.6]. In these regions, no significant change in SLC was found, except for the station of Kungsholmsfort. In the Bothnian Bay, the tide-gauge records of Oulu, Ratan, and Vaasa show coherent Hurst exponents close to 0.6 and strong significant unnatural change of trends. The MASLT are 2.7 mm/yr at Oulu tide gauge, 0.9 mm/yr at Ratan tide gauge, and 0.8 mm/yr at Vaasa tide gauge, or about 73%, 56%, and 57% of the observed sea level trend, respectively.

The Mumbai tide gauge (Figure 2c), the unique more than a century long sea level record in the Indian Ocean, presents a significant unnatural SLC ($\alpha \sim 0.6$). The MASLT is 0.7 mm/yr and represents 64% of the observed sea level trend. In this megacity, no significant subsidence caused by groundwater pumping, oil/gas extraction from coastal reservoirs, or by sedimentary compaction in the Gulf of Cambay has yet been demonstrated, and the unnatural sea level trend is probably induced by externally driven changes in the Indian Ocean currents.

On the west side of Australia (Figure 2c), the tide-gauge record of Fremantle has a $\alpha \sim 0.8$ and shows a strong significant unnatural SLC. The MASLT is 0.9 mm/yr, or about 47% of the observed sea level trend. The Fremantle tide gauge is located in the Perth Basin, where land subsidence has been reported in previous studies [*Belperio*, 1993; *Featherstone et al*., 2012; *Burgette et al*., 2013]. In contrast to Fremantle, the Sydney tide-gauge record from the eastern coast of Australia does not present statistically significant unnatural SLC ($\alpha \sim 0.9$). In this site, there is no noticeable tectonic activity, and the coastal subsidence has a slow rate [*Murray-Wallace and Belperio*, 1991].

3.2. Global Mean Sea Level

GMSLR06 displays a larger fluctuation exponent: $\alpha = 1.08$ against $\alpha = 0.83$ for GMSLR11 pointing to nonstationary fluctuations in GMSLR06 (as $\alpha > 1$, Figure 1b). The observed difference is probably due to the interannual and decadal variabilities that look to be more suppressed in GMSLR11 than in GMSLR06 (Figure 1a). Despite these differences, both GMSLR06 and GMSLR11 reveal a presence of a significant unnatural SLC of at least 1 and 1.3 mm/yr, respectively. This MASLT in GMSLR is in line with the results of *Jevrejeva et al*. [2009] who have modeled global sea level variations over the last 1000 years by using different climate forcing mechanisms with constraints on the model predictions to be close to GMSCL06 over the last 200 years. They have concluded that the global mean sea level was largely driven by anthropogenic factors, rapid increase of CO_2, and other greenhouse gases, since 1850. According to the *IPCC AR5* [2013], it is very likely that there is a substantial contribution from anthropogenic forcing to the GMSL rise since the 1970s due to the combination of ocean warming and mass loss of glaciers. Moreover, *Church et al*. [2013] have recently analyzed the relative contribution of different processes to changes in the rate of GMSL rise during the period 1900–2010 and found that not the whole 20th century sea level rise is necessarily externally forced. They have concluded that the observed increased rate of GMSL rise since 1990 is not a part of natural cycle but a direct response to the increased radiative forcing (both anthropogenic and natural) of the climate system. *Calafat and Chambers* [2013] have quantified the contribution of internal climate variability to the sea level for the period 1920–2011. They have found a statistically significant acceleration over 1952–2011 that appears to be the result of increasing greenhouse gas concentrations, along with changes in volcanic forcing and tropospheric aerosol loading. Therefore on a global scale, all of the works mentioned above show the emergence of a detectable signal in GMSL that can be attributed to anthropogenic influence.

4. Discussion and Conclusion

In this study, we were seeking to estimate the minimum rate of the anthropogenic sea level trend in the longest tide-gauge records and in the GMSL reconstructions. The results presented above are based on two principal hypotheses: First, we supposed that natural behavior of sea level consists of increases and decreases occurring with frequencies following a power law distribution. Second, we assumed that the anthropogenic contribution was very small in the past and is getting much stronger today. For simplicity, we approximated an anthropogenic trend over the past 100–150 years by a linear function. Detection and estimation of the minimum anthropogenic sea level trend were then reformulated as a statistical hypothesis testing problem (details in Lennartz and Bunde [2012]): We tested the hypothesis that the natural sea level fluctuations, modeled by long-term correlated time series with a Hurst exponent $\alpha > 0.5$, are superimposed by an unknown linear anthropogenic trend. A DFA2-based approach was applied to measure the Hurst exponent of GMSLR and of 59 tide-gauge records to detect the presence of the external sea level trend. This analysis provides statistical evidences that the observed SLC, at global and regional scales, is beyond its natural internal variability by exceeding the 99% confidence intervals of the statistics of *Lennartz and Bunde* [2009]. A strong external anthropogenic trend is at least 1 mm/yr in GMSLR that is more than half of the total observed sea level trend during the XXth century. Moreover, a strong external anthropogenic trend is detected in some of the world's cities: it contributes to the observed sea level rise at least as much as 67% in New York and more than 50% in Baltimore, San Diego, Galveston, Marseille, and Mumbai. The same goes along the south coast of the North Sea: a strong external anthropogenic trend contributes to the observed sea level rise more than 50% from Cuxhaven to Hoek Van Holland. In the extreme western part of the Baltic Sea a strong external anthropogenic trend contributes to the observed sea level rise more than 80% in Wismar, Gedser, Warnemunde, and Travemunde. Overall, the presence of significant anthropogenic trends was found in two thirds of the longest century-scale sea level records. It is worthwhile noting that records with strong persistence may have a large increase for natural reasons, but in this case we cannot exclude the presence of anthropogenic trends similar to those observed at other stations, because the natural trend might be also negative.

The mathematical method we used can only distinguish between long-term correlations and trends, but not the origin of trends. Thus, our analysis only reveals the minimum amount of (linear) trends, which cannot be associated with power law long-range memory. On the other hand, the power law distribution of sea level fluctuations does not exclude low frequencies, which can look similar to linear functions over the past

100–150 years. Consequently, if the natural behavior on low frequencies is stronger than estimated by the long-range memory model, then the outcome of our analysis must be corrected by this contribution. In other words, if the natural persistence would result in a stronger linear increase during the investigated period, the anthropogenic contribution would be lower, but if the natural trend would be negative, then the anthropogenic contribution should be even stronger. If, instead, the natural correlations are weaker than assumed by power law correlations, then also the anthropogenic contribution might be stronger. It means that in the last two cases the anthropogenic contributions would increase, and thus our lower bounds are still valid. It is only in the case of a strong natural (approximately linear) increase when our lower bounds need to be corrected downwards, but we consider this case as unlikely.

To conclude, it would be important to emphasize that in this study we searched, first, for the lower bounds of the anthropogenic trends assuming the natural origin of sea level fluctuations as a null hypothesis. By definition, the estimates of MASLT presented above are drawn from probabilistic considerations. Nevertheless, the high confidence level (99%) set in hypothesis testing ensures the reliability of the MASLT estimates. Now, attention of future studies should be focused on the attribution part of the work: what combination of external drivers is the most likely responsible for the observed local and regional sea level changes? What are the external anthropogenic drivers that dominate the observed unnatural SLC?

Acknowledgments

We acknowledge the PSMSL, Proudman Oceanographic Laboratory, U.K., for making available the tide-gauge records and Prof. R. Peltier of the University of Toronto, Canada, for the ICE-5G v1.3 model. We would like to thank M. Bos for providing estimations of spectral indices from *Bos et al.* [2013]. We also thank two anonymous referees for their very helpful comments and suggestions. This project was supported by the CECILE ANR CNRS project ANR-09-CEP-001-01. M. Becker is supported by a CNES/FSE fellowship.

The Editor thanks two anonymous reviewers for their assistance in evaluating this paper.

References

Agnew, D. C. (1992), The time-domain behavior of power-law noises, *Geophys. Res. Lett.*, *19*(4), 333–336, doi:10.1029/91GL02832.

Barbosa, S. M., M. E. Silva, and M. J. Fernandes (2008), Time series analysis of sea-level records: Characterising long-term variability, in *Nonlinear Time Series Analysis in the Geosciences*, pp. 157–173, Springer, Berlin Heidelberg, doi:10.1007/978-3-540-78938-3_8.

Becker, M., M. Karpytchev, M. Davy, and K. Doekes (2009), Impact of a shift in mean on the sea level rise: Application to the tide gauges in the Southern Netherlands, *Cont. Shelf Res.*, *29*(4), 741–749.

Becker, M., B. Meyssignac, C. Letetrel, W. Llovel, A. Cazenave, and T. Delcroix (2012), Sea level variations at tropical Pacific islands since 1950, *Global Planet. Change*, *80*, 85–98.

Belperio, A. P. (1993), Land subsidence and sea level rise in the Port Adelaide estuary: Implications for monitoring the greenhouse effect, *Aust. J. Earth Sci.*, *40*(4), 359–368.

Beretta, A., H. E. Roman, F. Raicich, and F. Crisciani (2005), Long-time correlations of sea-level and local atmospheric pressure fluctuations at Trieste, *Physica A.*, *347*, 695–703.

Bloomfield, P., and D. Nychka (1992), Climate spectra and detecting climate change, *Clim. Change*, *21*(3), 275–287.

Bos, M. S., S. D. P. Williams, I. B. Araújo, and L. Bastos (2013), The effect of temporal correlated noise on the sea level rate and acceleration uncertainty, *Geophys. J. Int.*, doi:10.1093/gji/ggt481.

Burgette, R. J., C. S. Watson, J. A. Church, N. J. White, P. Tregoning, and R. Coleman (2013), Characterizing and minimizing the effects of noise in tide gauge time series: Relative and geocentric sea level rise around Australia, *Geophys. J. Int.*, *194*(2), 719–736.

Calafat, F. M., and D. P. Chambers (2013), Quantifying recent acceleration in sea level unrelated to internal climate variability, *Geophys. Res. Lett.*, *40*, 3661–3666, doi:10.1002/grl.50731.

Cazenave, A., and W. Llovel (2010), Contemporary sea level rise, *Ann. Rev. Mar. Sci.*, *2*, 145–173.

Church, J. A., and N. J. White (2011), Sea-level rise from the late 19th to the early 21st century, *Surv. Geophys.*, *32*(4–5), 585–602.

Church, J. A., N. J. White, R. Coleman, K. Lambeck, and J. X. Mitrovica (2004), Estimates of the regional distribution of sea level rise over the 1950–2000 period, *J. Clim.*, *17*(13), 2609–2625.

Church, J. A., D. Monselesan, J. M. Gregory, and B. Marzeion (2013), Evaluating the ability of process based models to project sea-level change, *Environ. Res. Lett.*, *8*(1), 014051.

Davis, R. A. (2011), *Sea-Level Changes in the Gulf of Mexico*, Harte Research Institute for Gulf of Mexico Studies series, 1st ed., Texas A&M Univ. Press, College Station, Tex.

Featherstone, W. E., M. S. Filmer, N. T. Penna, L. M. Morgan, and A. Schenk (2012), Anthropogenic land subsidence in the Perth Basin: Challenges for its retrospective geodetic detection, *J. R. Soc. West. Aust.*, *95*(1), 53–62.

Feder, J. (1988), *Fractals, 1988*, Plenum Press, New York.

Hasselmann, K. (1993), Optimal fingerprints for the detection of time-dependent climate change, *J. Clim.*, *6*(10), 1957–1971.

Hegerl, G. C., H. von Storch, K. Hasselmann, B. D. Santer, U. Cubasch, and P. D. Jones (1996), Detecting greenhouse-gas-induced climate change with an optimal fingerprint method, *J. Clim.*, *9*(10), 2281–2306.

Hegerl, G. C., O. Hoegh-Guldberg, G. Casassa, M. P. Hoerling, R. S. Kovats, C. Parmesan, D. W. Pierce, and P. A. Stott (2010), Good practice guidance paper on detection and attribution related to anthropogenic climate change, in *Meeting Report of the IPCC Expert Meeting on Detection and Attribution of Anthropogenic Climate Change*, edited by T. F. Stocker et al., pp. 1–8, IPCC Working Group I Technical Support Unit, Univ. of Bern, Bern, Switzerland.

Holgate, S. J., A. Matthews, P. L. Woodworth, L. J. Rickards, M. E. Tamisiea, E. Bradshaw, P. R. Foden, K. M. Gordon, S. Jevrejeva, and J. Pugh (2013), New data systems and products at the permanent service for mean sea level, *J. Coast. Res.*, *288*, 493–504, doi:10.2112/JCOASTRES-D-12-00175.1.

Hughes, C. W., and S. D. P. Williams (2010), The color of sea level: Importance of spatial variations in spectral shape for assessing the significance of trends, *J. Geophys. Res.*, *115*, C10048, doi:10.1029/2010JC006102.

Hurst, H. E., R. P. Black, and Y. M. Simaika (1965), *Long-Term Storage: An Experimental Study*, Royaume-Uni., Constable, London, U. K.

IPCC AR5 (2013), Summary for policymakers, in *Climate Change 2013: The Physical Science Basis. Contribution of Working Group I to the Fifth Assessment Report of the Intergovernmental Panel on Climate Change*, edited by T. F. Stocker et al., Cambridge Univ. Press, Cambridge, U. K., and New York.

Jevrejeva, S., A. Grinsted, J. C. Moore, and S. Holgate (2006), Nonlinear trends and multiyear cycles in sea level records, *J. Geophys. Res.*, *111*, C09012, doi:10.1029/2005JC003229.

Jevrejeva, S., A. Grinsted, and J. C. Moore (2009), Anthropogenic forcing dominates sea level rise since 1850, *Geophys. Res. Lett.*, *36*, L20706, doi:10.1029/2009GL040216.
Kantelhardt, J. W., E. Koscielny-Bunde, H. H. Rego, S. Havlin, and A. Bunde (2001), Detecting long-range correlations with detrended fluctuation analysis, *Physica A*, *295*(3), 441–454.
Kolker, A. S., M. A. Allison, and S. Hameed (2011), An evaluation of subsidence rates and sea-level variability in the northern Gulf of Mexico, *Geophys. Res. Lett.*, *38*, L21404, doi:10.1029/2011GL049458.
Koscielny-Bunde, E., J. W. Kantelhardt, P. Braun, A. Bunde, and S. Havlin (2006), Long-term persistence and multifractality of river runoff records: Detrended fluctuation studies, *J. Hydrol.*, *322*(1), 120–137.
Lennartz, S., and A. Bunde (2009), Trend evaluation in records with long-term memory: Application to global warming, *Geophys. Res. Lett.*, *36*, L16706, doi:10.1029/2009GL039516.
Lennartz, S., and A. Bunde (2011), Distribution of natural trends in long-term correlated records: A scaling approach, *Phys. Rev. E*, *84*(2), 021129.
Lennartz, S., and A. Bunde (2012), On the estimation of natural and anthropogenic trends in climate records, in *Extreme Events and Natural Hazards: The Complexity Perspective*, *Geophys. Monogr. Ser.*, *196*, edited by A. S. Sharma et al., pp. 177–189, AGU, Washington, D. C.
Mandelbrot, B. B., and J. R. Wallis (1968), Noah, Joseph, and operational hydrology, *Water Resour. Res.*, *4*(5), 909–918.
Mandelbrot, B. B., and J. R. Wallis (1969), Some long-run properties of geophysical records, *Water Resour. Res.*, *5*(2), 321–340.
Maul, G. A., and D. M. Martin (1993), Sea level rise at Key West, Florida, 1846-1992: America's longest instrument record?, *Geophys. Res. Lett.*, *20*, 1955–1958, doi:10.1029/93GL02371.
Meyssignac, B., D. Salas, M. Becker, W. Llovel, and A. Cazenave (2012), Tropical Pacific spatial trend patterns in observed sea level: Internal variability and/or anthropogenic signature?, *Clim. Past Discuss.*, *8*(1), 787–802.
Miller, L., and B. C. Douglas (2007), Gyre-scale atmospheric pressure variations and their relation to 19th and 20th century sea level rise, *Geophys. Res. Lett.*, *34*, L16602, doi:10.1029/2007GL030862.
Mitchum, G. T., R. S. Nerem, M. A. Merrifield, and W. R. Gehrels (2010), Modern sea-level-change estimates, in *Understanding Sea-Level Rise and Variability*, edited by J. A. Church et al., pp. 122–142, Wiley-Blackwell, Oxford, U. K.
Morton, R. A., J. C. Bernier, and J. A. Barras (2006), Evidence of regional subsidence and associated interior wetland loss induced by hydrocarbon production, Gulf Coast region, USA, *Environ. Geol.*, *50*(2), 261–274.
Murray-Wallace, C. V., and A. P. Belperio (1991), The last interglacial shoreline in Australia—A review, *Quat. Sci. Rev.*, *10*(5), 441–461.
Nerem, R. S., D. P. Chambers, C. Choe, and G. T. Mitchum (2010), Estimating mean sea level change from the TOPEX and Jason altimeter missions, *Mar. Geod.*, *33*(S1), 435–446.
Peltier, W. R. (2004), Global glacial isostasy and the surface of the ice-age Earth: The ICE-5G (VM2) model and GRACE, *Annu. Rev. Earth Planet. Sci.*, *32*, 111–149.
PSMSL (2014), Permanent Service for Mean Sea Level, "Tide Gauge Data." [Available at http://www.psmsl.org/data/obtaining/.]
Rybski, D., and A. Bunde (2009), On the detection of trends in long-term correlated records, *Physica A*, *388*(8), 1687–1695.
Sallenger, A. H., K. S. Doran, and P. A. Howd (2012), Hotspot of accelerated sea-level rise on the Atlantic coast of North America, *Nat. Clim. Change*, *2*(12), 884–888.
Stammer, D., A. Cazenave, R. M. Ponte, and M. E. Tamisiea (2013), Causes for contemporary regional sea level changes, *Ann. Rev. Mar. Sci.*, *5*, 21–46.
Woodworth, P. L., N. Pouvreau, and G. Wöppelmann (2010), The gyre-scale circulation of the North Atlantic and sea level at Brest, *Ocean Sci.*, *6*(1), 185–190, doi:10.5194/os-6-185-2010.
Zorita, E., T. F. Stocker, and H. von Storch (2008), How unusual is the recent series of warm years?, *Geophys. Res. Lett.*, *35*, L24706, doi:10.1029/2008GL036228.
Zwiers, F. (2005), Detecting and attributing external influences on the climate system: A review of recent advances, *J. Clim.*, *18*(9).